Journal of Steroid Biochemistry and Molecular Biology 233 (2023) 106365

Contents lists available at ScienceDirect

Journal of Steroid Biochemistry and Molecular Biology

journal homepage: www.elsevier.com/locate/jsbmb

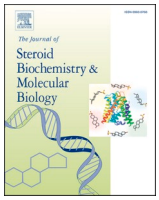

Small change – big consequence: The impact of C15-C16 double bond in a D-ring of estrone on estrogen receptor activity

Petr Vonka [a,b], Lucie Rarova [c], Vaclav Bazgier [d], Vlastimil Tichy [a], Tamara Kolarova [a], Jitka Holcakova [a], Karel Berka [d], Miroslav Kvasnica [b], Jana Oklestkova [b], Eva Kudova [e], Miroslav Strnad [b], Roman Hrstka [a,b,*]

[a] Research Centre for Applied Molecular Oncology, Masaryk Memorial Cancer Institute, Žlutý kopec 7, 656 53 Brno, Czech Republic
[b] Laboratory of Growth Regulators, Faculty of Science of Palacký University & Institute of Experimental Botany of the Czech Academy of Sciences, Šlechtitelů 27, 783 71 Olomouc, Czech Republic
[c] Department of Experimental Biology, Faculty of Science, Palacký University Olomouc, Šlechtitelů 27, 78371 Olomouc, Czech Republic
[d] Department of Physical Chemistry, Faculty of Science, Palacký University Olomouc, třída 17. listopadu 12, 771 46 Olomouc, Czech Republic
[e] Institute of Organic Chemistry and Biochemistry AS CR, Flemingovo náměstí 2, 166 10, Praha 6, Czech Republic

ARTICLE INFO

Keywords:
Estrogen receptor alpha
Docking of steroid library
Luciferase assay
Apoptosis
Mitochondrial membrane potential

ABSTRACT

Estrogen receptor alpha (ER) is a key biomarker for breast cancer, and the presence or absence of ER in breast and other hormone-dependent cancers decides treatment regimens and patient prognosis. ER is activated after ligand binding - typically by steroid. 2682 steroid compounds were used in a molecular docking study to identify novel ligands for ER and to predict compounds that may show anticancer activity. The effect of the most promising compounds was determined by a novel luciferase reporter assay. Two compounds, **7** and **12**, showing ER inhibitory activity comparable to clinical inhibitors such as tamoxifen or fulvestrant were selected. We propose that the inhibitory effect of compounds **7** and **12** on ER is related to the presence of a double bond in their D-ring, which may protect against ER activation by reducing the electron density of the keto group, or may undergo metabolism leading to an active compound. Western blotting revealed that compound **12** decreased the level of ER in the breast cancer cell line MCF7, which was associated with reduced expression of both isoforms of the progesterone receptor, a well-known downstream target of ER. However, compound **12** has a different mechanism of action from fulvestrant. Furthermore, we found that compound **12** interferes with mitochondrial functions, probably by disrupting the electron transport chain, leading to induction of the intrinsic apoptotic pathway even in ER-negative breast cancer cells. In conclusion, the combination of computational and experimental methods shown here represents a rapid approach to determine the activity of compounds towards ER. Our data will not only contribute to research focused on the regulation of ER activity but may also be useful for the further development of novel steroid receptor-targeted drugs applicable in clinical practice.

1. Introduction

Breast cancer is the most frequent malignancy in women. In total, 2261,419 new cases of female breast cancer were diagnosed worldwide in 2020, representing 11.7% of total cancer cases in that year and 24.5% of all newly diagnosed cancers among women. Female breast cancer led to the death of 684,996 patients worldwide, representing 6.9% of total cancer death and 15.5% of cancer death among women [1]. Although breast cancer screening programs reduce mortality through early diagnosis, further development of more effective diagnostics and therapeutics continues to be a hot topic.

Treatment decision of breast cancer patients is mostly associated

Abbreviations: ΔΨm, Mitochondrial transmembrane potential; AZD-9833, Camizestrant; BZM, Bortezomib; DMSO, Dimethyl sulfoxide; E1, Estradiol; E2, Estrone; ER, Estrogen receptor alpha; FLUC, Firefly luciferase; FLV, Fulvestrant; HER2, Human epidermal growth factor receptor 2; HTVS, High-throughput virtual screening; IHC4, Prognostic score for breast cancer subtypes based on immunohistochemical markers; MTT, 3-(4,5-dimethylthiazol-2-yl)− 2,5-diphenyltetrazolium bromide; PI, Propidium iodide; PR, Progesterone receptor; RAD-1901, Elacestrant; RLUC, Renilla luciferase; SERD, Selective estrogen-receptor downregulators; SERM, Selective oestrogen-receptor response modulators; TAM, Tamoxifen; VLM, Valinomycin.

* Corresponding author at: Research Centre for Applied Molecular Oncology, Masaryk Memorial Cancer Institute, Žlutý kopec 7, 656 53 Brno, Czech Republic.
E-mail address: hrstka@mou.cz (R. Hrstka).

https://doi.org/10.1016/j.jsbmb.2023.106365
Received 26 April 2023; Received in revised form 13 July 2023; Accepted 16 July 2023
Available online 17 July 2023
0960-0760/© 2023 The Authors. Published by Elsevier Ltd. This is an open access article under the CC BY license (http://creativecommons.org/licenses/by/4.0/).

with expression of four immunohistochemical markers; estrogen receptor α, progesterone receptor, human epidermal growth factor receptor 2 (hereafter referred to as ER, PR, HER2), and Ki-67 [2]. Based on them, breast cancer is divided into four intrinsic subtypes called IHC4 score that [3] includes luminal A, luminal B, HER2-enriched (also called HER2-positive (non-luminal)), and triple-negative (also called basal-like). This is consistent with a complementary approach based on gene expression divides breast tumors into five intrinsic subtypes including luminal A, luminal B, HER2-positive , basal-like and normal-like tumors [4,5]. Although gene expression profiling is not used in clinical laboratories as often as the IHC4 score, this classification may show a better prognostic outcome, shown for example in the NCIC.CTG MA.12 clinical trial that comprised pre-menopausal women with primary breast cancer treated by tamoxifen or placebo [6].

Approximately 70% of all patients with breast cancer are classified as ER-positive [7]. Activation of ER by estrogens has a pro-oncogenic effect, since ER functions as a transcription factor regulating the expression of many genes involved in cell cycle progression [8]. To abrogate ER activation by estrogens, small organic molecules have been developed to inhibit either estrogen production (aromatase inhibitors) or estrogen signaling (antiestrogens). Antiestrogens are usually steroids or steroid mimics that compete with endogenous estrogens for binding to ER and modify their activity as ligand-dependent regulators of transcription [9]. They can be divided into two classes differing in the mechanism of action.

The first class consists of selective estrogen-receptor response modulators (SERMs). These drugs are tissue-specific partial agonists of ER. In other words, they can show antiestrogenic or estrogenic effects depending on the tissue type. The first and the most common representative of this class is a derivative of triphenylethylene referred to as tamoxifen (TAM; formerly known as ICI 46,474 or Nolvadex; [10]). The antiestrogenic effect of TAM reduces the growth and development of ER-positive breast cancer [11,12]. Moreover, TAM supports the maintenance of bone mineral density in the lumbar spine and femur in postmenopausal women [13,14], and causes reduction of low-density lipoproteins, total cholesterol, and fibrinogen levels in postmenopausal women, which has a positive impact on the risk of coronary heart disease [15]. TAM belongs to the first generation of SERMs used for the treatment of patients with breast cancer. Due to clear benefits, second generation, e.g. raloxifene, and third generation SERMs, e.g. bazedoxifene, were developed and approved for clinical application [16].

The second class of antiestrogens encompasses selective estrogen-receptor downregulators (SERDs), also known as pure antiestrogens. These drugs cause a complete block of estrogen signaling. Fulvestrant (FLV; formerly known as ICI 182,780; Faslodex) was the first representative of this class [17]. FLV reduces the cellular level of ER by its degradation through the ubiquitin-proteasome pathway [18,19]. However, a disadvantage of FLV is its low oral bioavailability. Efforts to improve solubility led to the discovery of new SERDs (GSK compound, GW-5638, GW-7604, and GDC-0810). Unfortunately, subsequent clinical studies were discontinued due to severe side-effects. Nevertheless, other promising SERDs such as RAD-1901, AZD-9833, and GDC-9545 are currently being tested in clinical trials [20].

Despite the success of the aforementioned drugs, breast cancer remains a problem to many women and therefore considerable efforts are still being made to discover and develop new effective ER inhibitors. For this reason, we performed an *in silico* screen in our steroid compounds library, which led to the selection of 15 potential ER ligands. **7** and **12** were identified by the MTT assay measuring cellular metabolic activity as the most promising compounds showing significant cytotoxic effects. Following biological experiments confirmed in particular **12** as a potent inhibitor of ER. This compound shows high structural similarity with estrone (a natural activator of ER), except for the double bond in the D-ring of steroid backbone of compound **12**. Our results indicate that this small structural change exerts a significant inhibitory effect on ER activity comparable to routinely used commercial inhibitors such as TAM or FLV.

2. Materials and methods

2.1. Virtual screening of steroid compound library by molecular docking

The workflow of virtual screening using molecular docking was designed as a set of semi-automated steps, that include input data preparation, molecular docking and validation, interpretation and visualization of results. A set of in-house bash scripts was used for the preparation and validation of input/output data. The collection of steroid derivatives from the IOCB (Institute of Organic Chemistry and Biochemistry of the Czech Academy of Sciences) research group was used as the input database of ligands that needed conversion from paper into electronic form. All 3D structures of ligands were obtained with Marvin 5.10.3 [21], software which can be used for drawing, displaying and characterization of chemical structures, substructures and reactions. Two crystal structures were used as protein targets – ER complexed with the agonist genistein (PDBID: 1X7R; [22]) and with the antagonist 4-hydroxytamoxifen (PDBID: 3ERT; [23]). Polar hydrogens were added to all ligands and proteins with the AutoDock Tools [24] before docking. Autodock Vina 1.05 [25] was used for molecular docking of the ligand database to the protein targets. A 25 Å docking grid box was centered on the void original ligand location in the structure. The exhaustiveness parameter was set to default value 8. The highest energy of docking from multiple ligand positions were determined for each compound and these were used to rank ligands.

2.2. Cell culture

Human embryonic kidney cell line HEK293 and two human breast cancer cell lines, ER-positive MCF7 and ER-negative MDA-MB-231, were maintained in Dulbecco's modified Eagle's medium-high glucose (DMEM; Merck KGaA, Darmstadt, Germany). The medium was supplemented with 10% fetal bovine serum (FBS; Gibco, Thermo Fisher Scientific, Inc., Waltham, Massachusetts, USA), 100 U/ml penicillin, 0.1 mg/ml streptomycin (Biosera, Nuaille, France) and 2 mM L-pyruvate (Gibco, Thermo Fisher Scientific, Inc., Waltham, Massachusetts, USA) in a humidified incubator at 37 °C in 5% CO_2 atmosphere. All cell lines were obtained from American Type Culture Collection (ATCC), for the experiments we used cells in 5–20 passages.

2.3. Western blotting analysis

To analyse the level of selected proteins, MCF7 cells were seeded at a density of 300,000 cells/6 cm-plate and treated after 24 h. Compounds were applied at final concentrations as follows: 1 nM estradiol (E2; Sigma-Aldrich, St. Louis, USA), 2 μM TAM (Sigma-Aldrich, St. Louis, USA) or FLV (Sigma-Aldrich, St. Louis, USA), 10 nM bortezomib (BZM; Sellect Chemicals, Munich, Germany), 0.2 μM MG-132 (Sellect Chemicals, Munich, Germany), and 2 μM compound **12**. After treatments for 12, 24, 48, and 72 h, the cells were washed twice with PBS and harvested into PBS containing protease and phosphatase inhibitor cocktails (F. Hoffmann - Roche Ltd., Basel, Switzerland) and the number of cells measured (CASY cell counter, Cambridge Bioscience, Cambridge, UK). Cells were boiled in CSB buffer (10% glycerol, 1 M tris base pH 6.8, 2% bromphenol blue, 20% SDS, 5% β-mercaptoethanol). Equal amounts of total proteins were applied on 10% SDS polyacrylamide gels, followed by transfer onto nitrocellulose membranes. Membranes were blocked in 5% non-fat milk in PBS supplemented with 0.1% Tween-20 and labeled overnight with primary antibodies: estrogen receptor α (#ab16660, Abcam, Cambridge, UK), progesterone receptor (#NCL-L-PGR-312, Leica Biosystems Newcastle Ltd., Newcastle Upon Tyne, UK), and β-actin C4 (#sc-47778, Santa Cruz Biotechnology, Dallas, Texas, USA) as a loading control. After washing with PBS supplemented with 0.1%

Tween-20, membranes were incubated for 1 h at room temperature with appropriate HRP-conjugated secondary antibody RAM-Px (#P0161, lot 20044780; Dako, Glostrup, Denmark) or SWAR-Px (#P0217, lot 20020160; Dako, Glostrup, Denmark). Specific protein signals were detected with ECL reagents (Amersham Pharmacia Biotech, Buckinghamshire, UK) using G-BOXChemi XX6 System (Syngene, Cambridge, UK). At least three independent experiments were performed.

2.4. Development of dual Luciferase assay

2.4.1. Dual luciferase recombinant vector construction

The full-length *firefly luciferase* (*FLUC*) gene with a promoter containing SV40 early enhancer with three estrogen-responsive elements (ERE) and three estrogen-related responsive elements (ERRE) was amplified by polymerase chain reaction (PCR) from 3xERRE/ERE-luciferase vector (Addgene Europe, Teddington, UK) using the following forward primer with an *Eco*RI restriction enzyme site (5′-CCGATCGAATTCCGCAATAAAATATCTTTATTT-3′) and the reverse primer with *Xho*I restriction enzyme site (5′-CCGCCGCTCGAGTTGTTTATTGCAGCTTATAAT-3′). The *FLUC* fragment was subcloned into pcDNA3 (Invitrogen, Carlsbad, California, USA) and verified by Sanger sequencing (Eurofins Genomics GmbH, Ebersberg, Germany). The full-length *renilla luciferase* (*RLUC*) gene was cut by restriction enzymes *Hind*III and *Bam*HI from the pRL-TK vector (Promega Corporation, Madison, Wisconsin, USA) and inserted into the prepared pcDNA3 vector with the *FLUC* gene. Correct insertion of *RLUC* was verified by sequencing.

2.4.2. Nucleofection of the cells

HEK293 cells were seeded in a 6 ml plate at 50% confluence 24 h prior to transfection in DMEM without antibiotics. The nucleofection was performed according to the manufacturer's instructions using Amaxa Cell Line Nucleofector (Lonza Cologne AG, Cologne, Germany). 2 μg vector DNAs were used to transfect 1×10^6 cells and the mass ratio of pcDNA3_hERα (plasmid with an inserted gene coding for human estrogen receptor alpha) and pcDNA3_FLUC_RLUC was 1:1. Control cells were transfected with either pcDNA3 or a combination of pcDNA3_hERα and pcDNA3. Transfected cells were seeded in 96-well plates at a density of 10,000 cells/well.

2.5. Dual luciferase reporter gene assay

The dual luciferase assay was used to analyse the effect of the compounds on ER activity. 24 h after plating luciferase reporter cells in DMEM medium without phenol red and supplemented with dialysed FBS, drugs were applied at the following final concentrations: 1 nM estrone (E1; Sigma-Aldrich,), 1 nM E2 (Sigma-Aldrich), 10 μM TAM (Sigma-Aldrich), 10 nM FLV (Sigma-Aldrich), and 1 μM tested steroid compounds. 24 h after the treatment, medium containing the drugs was removed and cells were seeded in a 96-well plate and then washed two-times using PBS (50 μl/well). Passive lysis buffer (Promega Corporation, Madison, Wisconsin, USA) was added (25 μl/well) and the plate was shaken at 4 °C for 15 min. FLUC measurement buffer (0.1 M tris base (pH 7.8), 15 mM $MgSO_4$, 4 mM EGTA, 1 mM ATP, 1 mM DTT, 0.2 mM D-luciferin sodium salt) was added into each well and FLUC bioluminescence was measured on a multifunctional microplate reader Infinite M1000 Pro (Tecan Group Ltd., Männedorf, Switzerland) (volume of FLUC buffer: 100 μl/well; filter: GREEN1 (560 nm); integration time: 10,000 ms; delay: 2000 ms). 300 mM EDTA acid (25 μl/well; 5 min incubation) was added to stop the FLUC signal. RLUC measurement buffer (13.4 mM KH_2PO_4 (pH 7.6), 86.6 mM K_2HPO_4, 0.5 M NaCl, 1 mM EDTA acid, 0.4 μM coelenterazine) was added and RLUC bioluminescence was determined (volume of RLUC buffer: 100 μl/well; filter: BLUE (480 nm); integration time: 10,000 ms; delay: 2000 ms) on a multifunctional microplate reader Infinite M1000 Pro (Tecan Group Ltd., Männedorf, Switzerland). The optimal functionality of our newly developed luciferase reporter system was verified by RT-qPCR analysis of two selected ER-regulated genes PGR and TFF1 in the presence and absence of E2 (Fig. SI-1).

2.6. MTT assay

This experimental approach was modified from [26]. Briefly, due to growth rate and size, MCF7 cells were seeded in 96-well plates at a density of 8000 cells/well and MDA-MB-231 cells at a density of 4000 cells/well. The next day, the cells were exposed to all tested compounds diluted in DMSO at a final concentration range of 0–75 μM (each in pentaplicates). Metabolic activity was measured after 72 h treatment using MTT (3-(4,5-dimethylthiazol-2-yl)− 2,5-diphenyltetrazolium bromide) assay; 20 μl MTT solution from the stock (2.5 mg/ml) was added and cells were incubated in a CO_2 incubator in the dark for 3 h. The medium was removed and formazan crystals were dissolved in 50 μl of DMSO per well. Absorbance was read at 595 nm using a multifunctional microplate reader Infinite M1000 Pro (Tecan Group Ltd., Männedorf, Switzerland). Data were analysed with GraphPad Prism 8 and expressed as IC_{50} values (compound concentrations that are responsible for 50% inhibition). Error bars were calculated as standard deviation (SD). At least three independent experiments were performed.

2.6.1. Crystal violet assay

MCF7 and MDA-MB-231 cells were seeded into 12-well plates at a density of 30,000 and 10,000 cells/well, respectively. The next day, the cells were exposed to all tested compounds diluted in DMSO at the following final concentrations: 2 μM TAM (Sigma-Aldrich), 2 μM FLV (Sigma-Aldrich), and 2 μM compound **12**. After 7 days of incubation, the medium was removed and cells were immediately stained with the solution of crystal violet (0.05 g crystal violet, 2.7 ml 37% formaldehyde, 10 ml 10 × PBS, 1 ml methanol, 86.3 ml H_2O) for 20 min at room temperature. Adherent stained cells were dissolved using 2% SDS. Absorbance was measured at 595 nm using a multifunctional microplate reader Infinite M1000 Pro (Tecan Group Ltd., Männedorf, Switzerland). Data were analysed with GraphPad Prism 8. Error bars were calculated as standard deviation (SD). At least three independent experiments were performed.

2.6.2. Cell cycle determination

To determine the effect of compound **12** on the cell cycle, MCF7 and MDA-MB-231 cells were seeded at a density of 300,000 cells/6 cm-plate and treated after 24 h. Compounds were applied at final concentrations as follows: compound **12** at three different final concentrations (1 μM, 2 μM, and 3.6 μM) and 10 μM cisplatin (CSPT; EBEWE Pharma Ges.m.b.H., Unterach, Austria) was used as a positive control (blocks cell cycle at the G2 phase). Cells were incubated with these compounds for 24 h, 48 h, and 72 h at 37 °C. The cells were then washed twice with PBS and fixed in 70% ethanol overnight at 4 °C. The cells were then stained with 10 μg/ml of propidium iodide (PI) supplemented with 100 μg/ml RNase A (Sigma-Aldrich) at room temperature for 30 min in the dark. After incubation, the samples were measured with a flow cytometer (FACS Verse, BD Biosciences, Franklin Lakes, New Jersey, USA) and the cell cycle was evaluated using BD FACSuiteTM software v1.0.6 (BD Biosciences, San Jose, California, USA). In total, 10,000 events were analysed for each sample.

2.7. JC-1 staining

2.7.1. Flowcytometry analysis

This experimental approach was adopted from [27]. Briefly, JC-1 (5,5′,6,6′-tetrachloro-1,1′,3,3′-tetraethyl-benzimidazolylcarbo-cyanin iodide) dye was used to analyse mitochondrial depolarization. JC-1 dye occurs as monomers in the cytoplasm, but it creates aggregates after passing through the mitochondrial membrane. Both structures are characterized by different fluorescent features. The excitation

wavelength for JC-1 dye is 488 nm. The emission wavelength for monomers is 535 nm (green fluorescence), but the emission wavelength for aggregates is 595 nm (orange-red fluorescence).

To determine the effect of compound **12** on mitochondrial membrane depolarization, MCF7 or MDA-MB-231 cells were seeded at a density of 300,000 cells/6 cm-plate and treated after 24 h. Compounds were applied at final concentrations as follows: compound **12** at three different final concentrations (1 μM, 2 μM, and 3.6 μM) and 10 μM valinomycin (VLM; Molecular probes, Eugene, Oregon, USA) as a positive control of mitochondrial depolarization. Cells were incubated with the applied compounds for 4 h at 37 °C. Then, the cells were harvested by trypsin, washed with PBS and treated with JC-1 dye (Invitrogen, Carlsbad, California, USA) at a final concentration of 5 μg/ml for 20 min in the dark at 37 °C. Cells were held on ice and immediately subjected to flow cytometry (FACS Verse, BD Biosciences, Franklin Lakes, New Jersey, USA). A total of 10,000 events were analysed for each sample.

2.7.2. Spectrophotometry analysis

MCF7 or MDA-MB-231 cells were seeded in 96-well plates at a density of 15,000 cells/well overnight. The next day, cells were exposed to compounds at final concentrations as follows: compound **12** at three different concentrations (1 μM, 2 μM, and 3.6 μM) and 10 μM VLM (Molecular probes, Eugene, Oregon, USA) for 4 h at 37 °C. After that, the cells were washed twice with PBS and stained with JC-1 dye (Invitrogen, Carlsbad, California, USA) at a final concentration of 5 μg/ml for 20 min in the dark at 37 °C. JC-1 fluorescence (the red signals of JC-1 monomers: Ex. 488/5 nm, Em. 590/5 nm; the green signals of JC-1 aggregates: Ex. 488/5 nm, Em. 530/5 nm) was read on a multifunctional microplate reader Infinite M1000 Pro (Tecan Group Ltd., Männedorf, Switzerland) using the following settings: reading mode of the bottom, gain setting of the optimal, flash number of 50, flash frequency of 400 Hz, settle time of 50 ms, and multiple reads per well (circle type and 4 ×4 size, when only four values from the center of each well were taken to analyse results).

2.8. Annexin V–Fluorescein Isothiocyanate (FITC)/Propidium Iodide (PI) binding assay

To perform analysis using a flow cytometer, MCF7 or MDA-MB-231 cells were seeded at a density of 300,000 cells/6 cm-plate and treated 24 h later. Compounds were applied at final concentrations as follows: compound **12** at three different concentrations (1 μM, 2 μM, and 3.6 μM) and CSPT (EBEWE Pharma Ges.m.b.H., Unterach, Austria) at 100 μM for MCF7 cells or 250 μM for MDA-MB-231 cells. Cells were incubated for 12 h at 37 °C, harvested by acutase, washed twice with PBS, centrifuged at 225g for 5 min, and resuspended in 100 μl Annexin V Binding buffer (10 mM HEPES/NaOH, pH 7.4; 14 mM NaCl; 2.5 mM $CaCl_2$) supplied with FITC-labeled Annexin V (BioLegend, San Diego, USA) and PI. The cells were gently vortexed and incubated for 15 min at room temperature in the dark. After incubation, 400 μl of Annexin V Binding buffer was added. Stained cells were held on ice and immediately measured by flow cytometry (FACS Verse, BD Biosciences, Franklin Lakes, New Jersey, USA).

2.9. Statistics

Student's unpaired t test was applied with the following settings: confidence level: 95%; experimental design: unpaired; Gaussian distribution: yes, parametric test; choose test: unpaired t test; P value: Two-tailed; P value style: GP (* < 0.05, ** < 0.01, *** < 0.001, **** < 0.0001, ns = non-significant). The statistical analysis was performed using GraphPad Prism version 8.0.1 for Windows (GraphPad Software, La Jolla California USA, www.graphpad.com).

3. Results

3.1. Library screening

Molecular docking was used for the virtual screening of steroid compounds from our library, which contains 2682 compounds. ER with the agonist genistein (PDB ID: 1X7R; [22]) and its inhibitor 4-hydroxytamoxifen (PDB ID: 3ERT; [23]) were used as the protein crystal structures for molecular docking. We identified 15 compounds (Fig. 1) that could be ER inhibitors according to their binding energies (Table SI-1). The effect of these compounds on the metabolic activity of MCF7 cells was analyzed using the MTT assay. Two compounds significantly inhibited the metabolic activity of MCF7 cells (Table SI-1), compound **7** (IC_{50} 4.6 ± 0.5 μM) and compound **12** (IC_{50} 3.6 ± 0.16 μM).

3.2. Comparison of chemical structures

The chemical structures of compound **7** (3α-hydroxy-5α-androst-15-en-17-one; [28]) and compound **12** (3-hydroxyestra-1,3,5(10),15-tetraen-17-one; International Publication Number of Patent: WO 2015/040051 A l [29]) demonstrate a high level of similarity with natural ER ligands such as E2 or E1 and the tested compound denoted as compound **10** (3α-hydroxy-5α-androstan-17-one; [30]). The structures of both compound **7** and compound **10** have an androstane skeleton with 3α-hydroxy configuration, which means that the aromatic ring is absent and both compounds have a C-18 methyl group in contrast to the structure of E1 (Fig. 2A). In addition, a double bond in a D-ring conjugated with a C17 oxo group is a shared motif of compound **7** and compound **12**. These findings show that the double bond in the D-ring distinguishes ER antagonists (compound **7** and compound **12**) from their metabolically inactive structure analogs (compound **10** and E1).

3.3. The effect of compounds 7, 10, and 12 on ER activity

To confirm the effect of these compounds on the activity of ER as a transcription factor, we used a dual-luciferase assay based on a bicistronic luciferase vector coding RLUC showing constitutive expression, and FLUC inducible in response to ER activation. The ratio of both signals (FLUC/RLUC) in control untreated cells therefore represents the basal ER activity. Moreover, the comparison of this ratio with the ratio obtained from cells treated with a tested compound indicates whether the compound acts as an agonist (e.g. E1, E2) or an antagonist (e.g. FLV, TAM) of ER. Representative results are shown in Fig. 2B (three independent measurements are shown in Fig. SI-2). From our selected compounds, compound **12** in particular significantly inhibited ER transcriptional activity. Therefore, only compound **12** was selected for further experiments and analysed more in detail. We first tested the activity of compound **12** at various concentrations without and with the presence of E2 to determine whether, consistent with molecular docking, the compound can inhibit ER activity by direct displacing E2 from the ER binding cavity (Fig. SI-3). We observed that increased concentrations of **12** clearly decreased ER activity both in cells cultured without addition of E2 (Fig. SI-3A) and cells pre-treated with E2 (Fig. SI-3B).

3.4. The impact of steroid derivative 12 on levels of ER and PR

Based on dual-luciferase assay data, we have analysed the effect of **12** on protein levels of ER and PR (Fig. 3A, Fig. SI-4). Treatment of MCF7 cells with **12** caused a decrease in ER level, especially in shorter periods, which was associated with a clear reduction of both PR isoforms. However, longer exposure to **12** was associated with a modest increase in the levels of both ER and PR protein isoforms. TAM (SERM) induced the level of ER but decreased the levels of both PR isoforms at all monitored periods, which corresponds to an inhibitory effect of TAM on the transcription of estrogen-responsive genes. In contrast, treatment with FLV (SERD) decreased ER levels, which in turn led to reduced

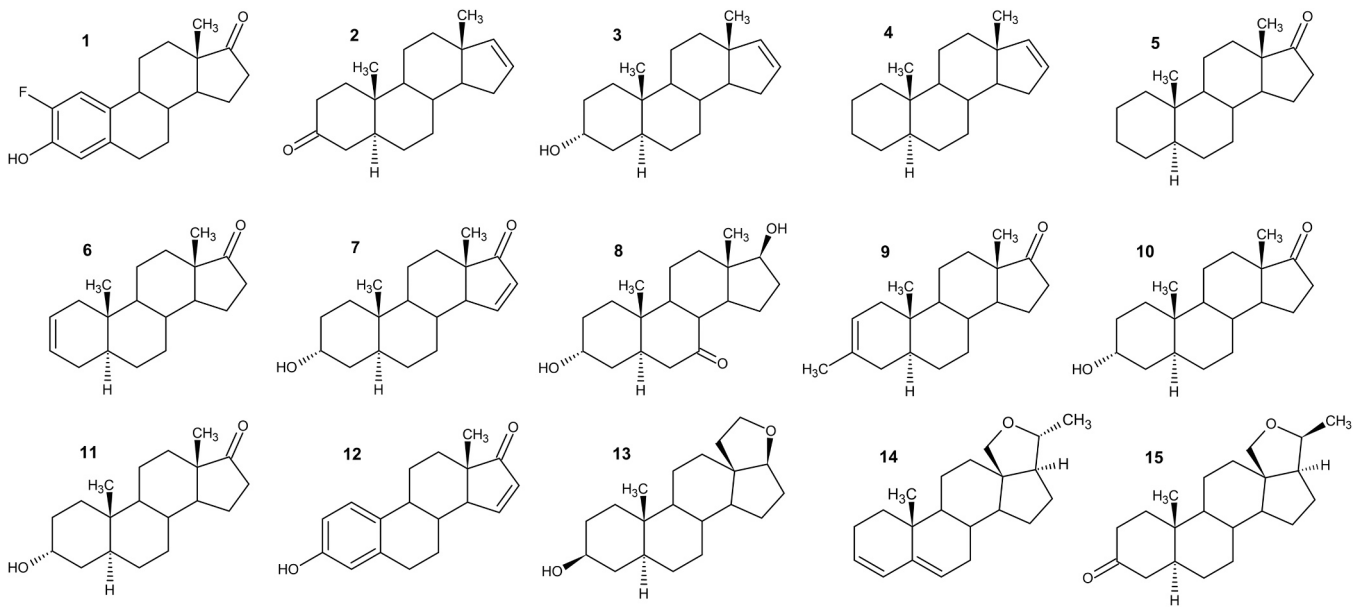

Fig. 1. Potential ER ligands. Molecular docking was used for virtual screening of the steroid compounds library to identify potential ligands of ER. Based on binding affinity values, 15 compounds were chosen for further analysis. ChemSketch software (ACD/ChemSketchTM for Academic and Personal Use; online available at : https://www.acdlabs.com/resources/free-chemistry-software-apps/chemsketch-freeware/; Advanced Chemistry Development, Inc., Toronto, Ontario, Canada) was used for drawing all steroid structures shown in this work.

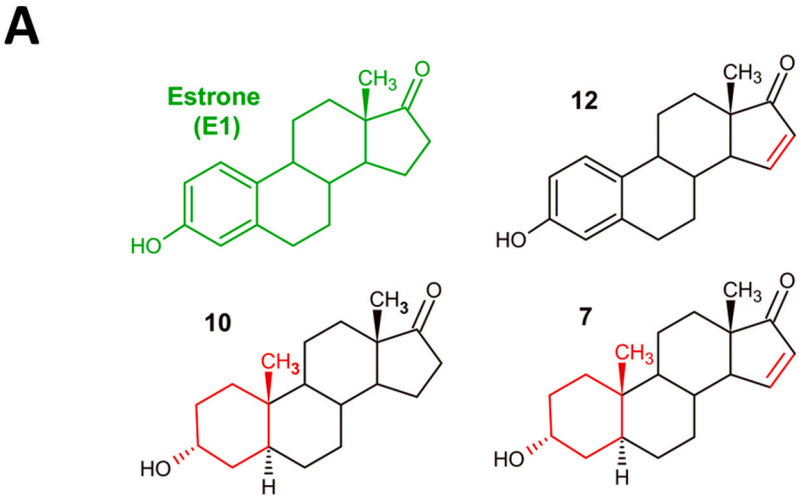

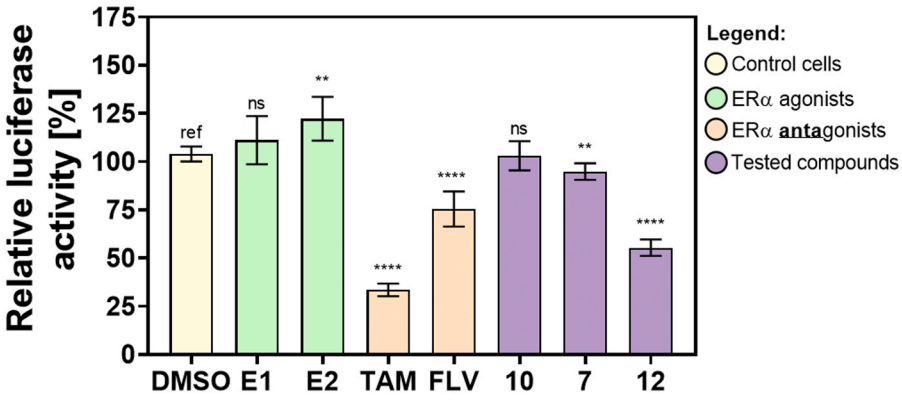

Fig. 2. Impact of selected compounds on ER. (A) STRUCTURES OF SELECTED COMPOUNDS. Differences in the structures of the tested compounds are highlighted in the red, structure of E1 is in green. (B) DETERMINATION OF ER ACTIVITY. The yellow bar represents control (untreated cells) which reflects the basal activity of ER, green bars for ER agonists, orange bars represent ER antagonists, and violet bars represent our tested compounds. Results are given as the arithmetic mean with standard deviation of the signal ratios of the two luciferases, and the arithmetic mean of the control cells was set as a value of 100%. The experiment was independently repeated three times (Fig. SI-2) and five technical replicas were used to determine each experimental value.

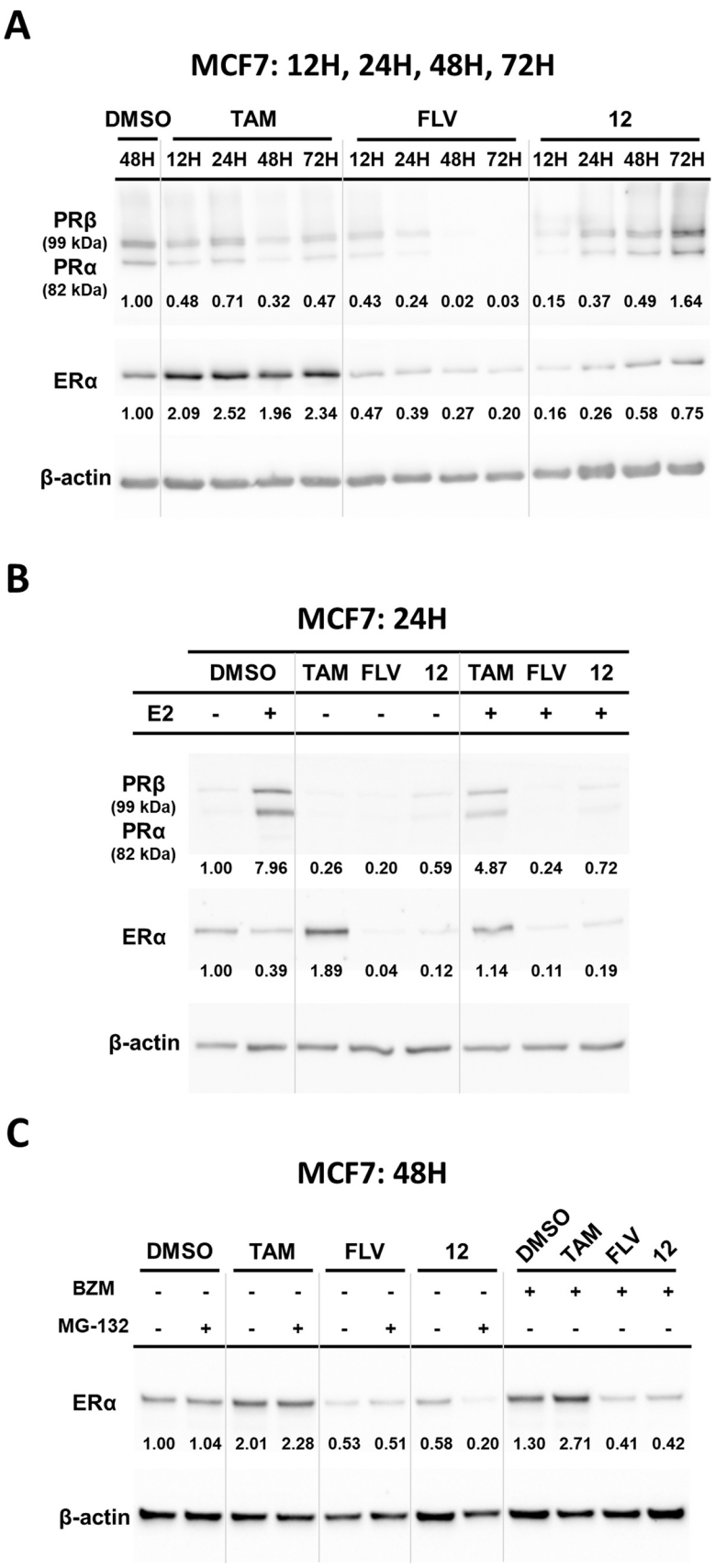

Fig. 3. Compound 12 effect on ER and PR levels. (A) WESTERN BLOTTING ANALYSIS OF ER AND PR. MCF7 cells were treated with DMSO, TAM, FLV, and 12. TAM and FLV were used as positive controls. The levels of ER and PR were determined at the indicated time points by western blotting analysis. The experiment was independently repeated three times with a similar trend (Fig. SI-4). β-actin was used as a loading control. Values represent the fold change of the relative density of protein bands normalised to β-actin, with respect to the relative density of control cells at 48 h which was set to 1.00. ImageJ software [31] was used to analyse protein levels. (B) WESTERN BLOTTING ANALYSIS OF ER AND PR IN RELATION TO THE PRESENCE OF E2. MCF7 cells were cultivated in the medium with and without E2 and exposed to TAM, FLV, and 12 for 24 h as indicated. The experiment was independently repeated three times with a similar trend (Fig. SI-5). β-actin was used as the loading control. All values represent the fold change of the relative density of protein bands normalised to β-actin, with respect to the relative density of control cells that was set to 1.00. ImageJ software [31] was used to analyse protein levels. (C) MECHANISM RESPONSIBLE FOR DECREASED ER LEVEL. MCF7 cells were treated with combinations of tested steroid compounds (TAM, FLV, or 12) and proteasome inhibitors (BZM or MG-132). Levels of ER were determined after 24 h (Fig. SI-6) and 48 h (shown in this figure) by immunochemical analysis. β-actin was used as the loading control. All values represent the fold change of the relative density of protein bands normalised to β-actin, with respect to the relative density of control cells that was set to 1.00. ImageJ software [31] was used to analyse protein levels.

transcription of estrogen-responsive genes including PR (Fig. 3A, Fig. SI-4). Compound **7** affected levels of ER and PR (Fig. SI-4) similarly to **12** but this effect was weaker.

The effect of **12** on protein levels of ER and PR isoforms was also analysed with respect to the presence of E2 in culture medium (Fig. 3B, Fig. SI-5). The presence of E2 itself decreased ER level but simultaneously induced PR expression confirming its agonistic effect on ER. Importantly, in cells cultured in E2-containing medium and exposed to **12**, we observed a clear decrease in both ER and PR levels to a similar extent as in response to FLV treatment, indicating that **12** has a significantly higher affinity for ER compared to E2 and thus effectively blocks its agonist activity towards this receptor and even reduces levels of the receptor.

To investigate in detail the mechanism responsible for the decrease in ER after treatment with **12**, we exposed MCF7 cells to this drug in combination with the proteasome inhibitors MG-132 or BZM. Combined treatment resulted in a decreased level of ER (Fig. 3C, Fig. SI-6), indicating that **12** does not induce degradation of ER by the proteasome as observed for FLV.

3.5. Compound 12 targets mitochondria

Many drugs exhibit dual or even multiple mechanisms of action. For instance, the non-genomic cytotoxic activity of TAM is caused by its accumulation in mitochondria and the endoplasmic reticulum [32,33]. In mitochondria, TAM and its metabolites affect the function of the electron transport chain, especially mitochondrial complex I [32] and complex III [34]. Therefore, the effect of **12** on ER-negative MDA-MB-231 breast cancer cells was also studied. Metabolic assay was used to analyse dose-dependent effects of studied compounds.

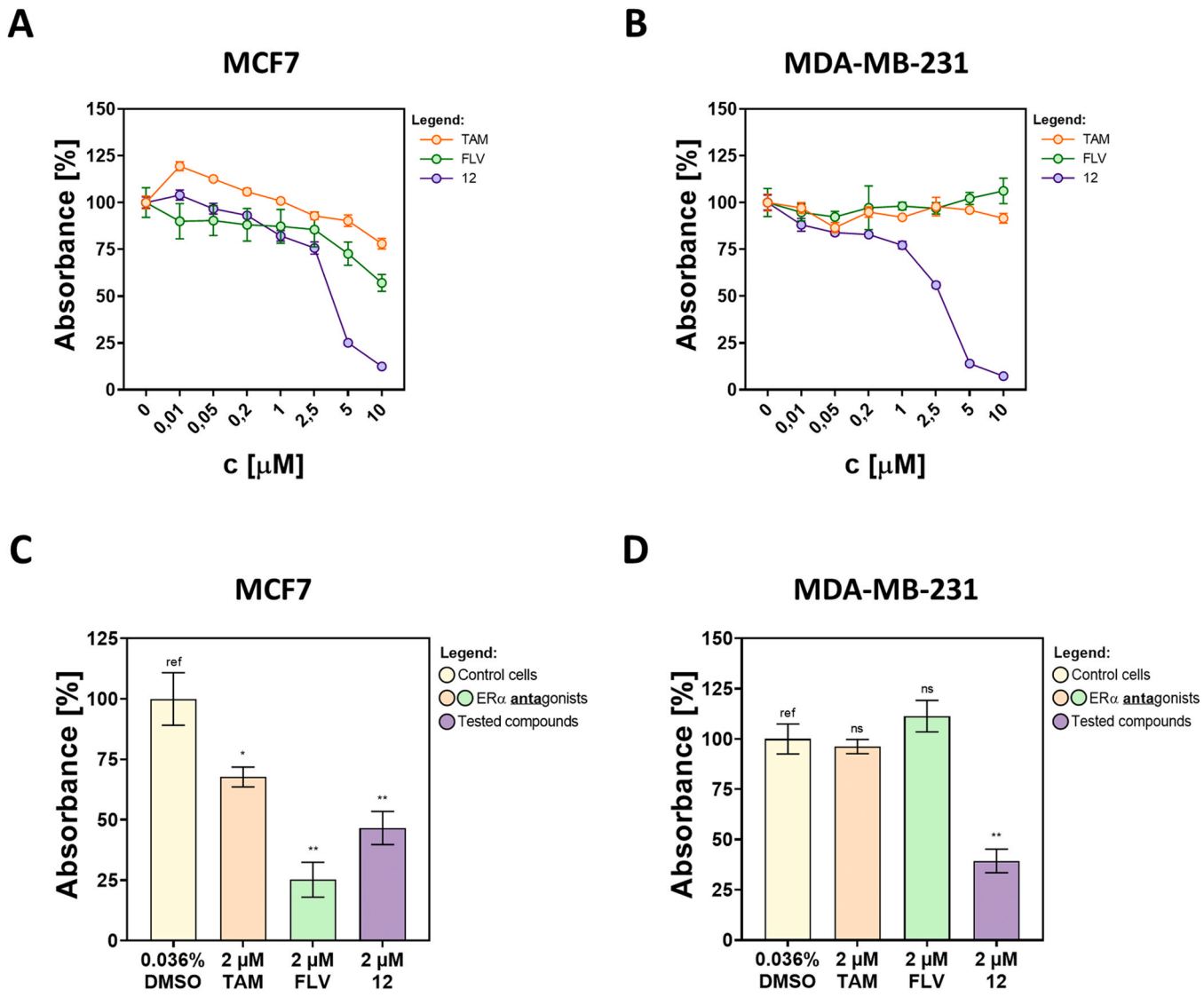

Fig. 4. Impact of tested compounds on cell viability. (A) MCF7 and (B) MDA-MB-231 cells were treated for 72 h with TAM (orange lines), FLV (green lines), or 12 (violet lines) to describe their effect on the metabolic activity using MTT assay. Representative results are shown as the arithmetic mean of absorbance with the standard deviation, whereas the arithmetic mean of control cells treated only with DMSO alone was set as 100%. The experiment was repeated at least three times for both cell lines (Fig. SI-7) and five technical replicates were used to determine each experimental value. GraphPad Prism version 8.0.1 for Windows (GraphPad Software, La Jolla, California, USA, www.graphpad.com) was used to analyse the obtained data. As an alternative to MTT assay, the effect of TAM (orange bars), FLV (green bars) and 12 (violet bars) on the proliferation of (C) MCF7 and (D) MDA-MB-231 cells was determined after 7 days of incubation using the crystal violet staining. Representative results are shown as the arithmetic mean of absorbance with the standard deviation, whereas the arithmetic mean of control cells (yellow bars) treated only with DMSO alone was set as 100%. The experiment was repeated at least three times for both cell lines (Fig. SI-8) and five technical replicates were used to determine each experimental value. GraphPad Prism version 8.0.1 for Windows (GraphPad Software, La Jolla, California, USA, www.graphpad.com) was used to analyse the obtained data.

Indeed, MTT assay revealed that **12** exhibits cytotoxicity towards these cells (IC_{50} = 4.6 ± 0.6 μM) at doses similar to MCF7 cells (IC_{50} = 3.6 ± 0.16 μM) (Figs. 4A and 4B, Fig. SI-7). Since proliferation assays with longer incubation times are more indicative of viability effects than MTT assays after 72 h, we used a crystal violet staining assay with an incubation time of 7 days (Figs. 4C and 4D, Fig. SI-8). In response to TAM and FLV as well as compound **12**, we observed a significant decrease in proliferation in ER-responsive MCF7 cells over this time period. On the other hand, even prolonged incubation had no significant effect in MDA-MB-231 cells, in which only compound **12** was effective. This is an important finding, since MDA-MB-231 cells do not express ER as compared to ER-positive MCF7, which indicates the presence of another mechanism through which **12** exerts its cytotoxic activity.

To test whether **12** directly targets mitochondria, we analysed changes in mitochondrial membrane potential (ΔΨm), which are usually caused by the interactions of small organic compounds, e. g. MitoTam, with mitochondrial structures [35]. The cationic fluorescent JC-1 dye was used in combination with optical detection by flow cytometry. Untreated cells are characterised by polarised mitochondria, as revealed by the high red fluorescence of JC-1 aggregates. Treatment with **12** caused a shift from the upper left to the lower right corner of the contour plot, reflecting the changes in ΔΨm (Fig. SI-9). The impact of **12** was detected for both MCF7 (Fig. SI-9) and MDA-MB-231 (Fig. 5 A, Fig. SI-9) cell lines.

In parallel, we used spectrophotometric analysis to determine the ratio of the red and the green JC-1 fluorescent signals (Fig. 5B; Fig. SI-10). Treatment with VLM as well as **12** caused a significant decrease in the ratio of JC-1 fluorescent signals compared to control untreated cells and confirmed mitochondria as the molecular target of **12** in both cell lines.

3.6. Apoptosis and cell cycle analysis

ΔΨm is essential for mitochondrial homeostasis and its decrease is commonly associated with mitochondrial dysfunction and is considered one of the early signs of apoptosis [36]. Thus, a PI flow cytometric assay in conjunction with Annexin V was applied to determine whether cells are viable, apoptotic, or necrotic due to differences in plasma membrane integrity and permeability. MCF7 (Fig. 6A; Fig. SI-11) and MDA-MB-231 (Fig. 6B; Fig. SI-11) cells were exposed to **12** in three different concentrations of 1 μM, 2 μM, and 3.6 μM. At lower concentrations (1 μM and 2 μM), **12** did not induce apoptosis in either cell line. The highest dose of **12** (3.6 μM) induced programmed cell death, as shown by an increased proportion of late apoptotic and necrotic cells.

Since ER is implicated in the regulation of cellular proliferation [37], we also analysed the effect of **12** on the cell cycle. Interestingly, no significant effect of **12** on the cell cycle of MCF7 cells (Fig. SI-12) was observed. However, cell cycle arrest at G2/M was seen in ER-negative MDA-MB-231 cells (Fig. 6C, Fig. SI-13) exposed to **12** in all incubation periods (24, 48, and 72 h).

4. Discussion

TAM and FLV are frequently used in clinical practice, however, the development of new antiestrogens with improved properties is still ongoing. Some antiestrogen-based drugs are currently in clinical trials,

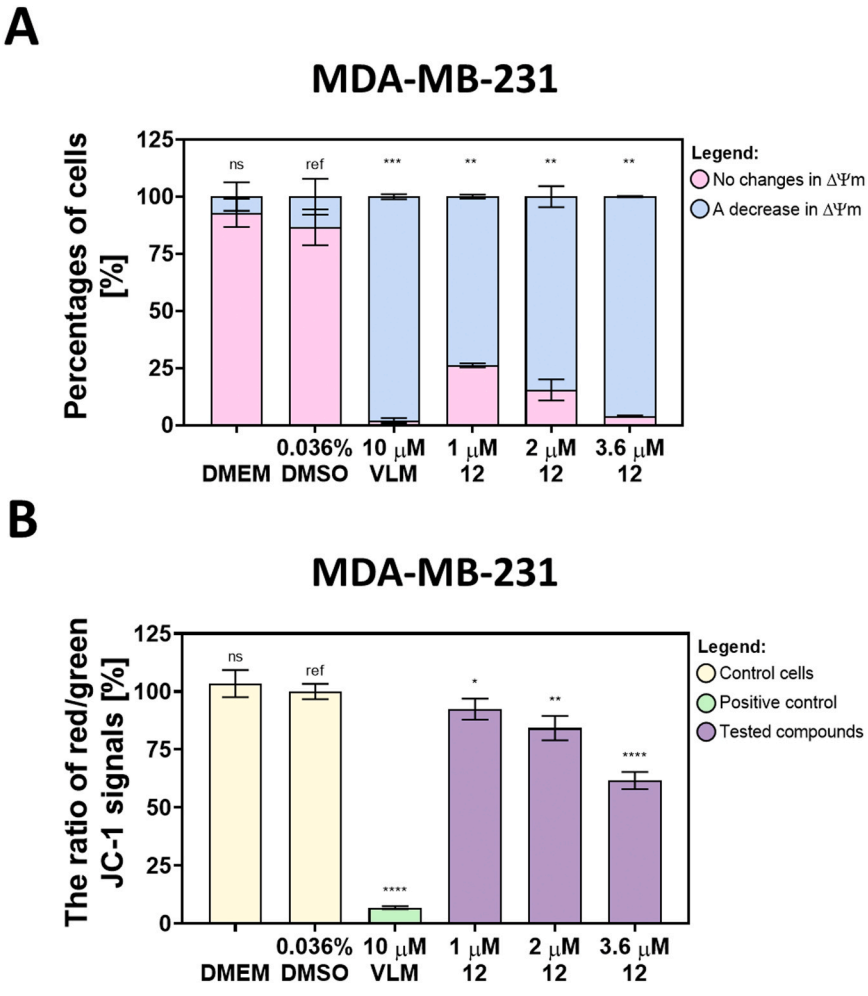

Fig. 5. ΔΨm determination. **(A, B)** Changes in ΔΨm were performed using JC-1 staining. MDA-MB-231 cells were treated with three concentrations of **12** and VLM as a positive control. **(A)** FLOW CYTOMETRY. Results are shown as stacked bar plots describing percentage changes in ΔΨm. Individual graphs are displayed in Fig. SI-9. Experimental data are presented as the arithmetic mean of three independent experiments with standard deviation, where the arithmetic mean of DMSO-treated control cells was set as 100%. The percentages of cells in the quadrants were determined using BD FACSuite™ software v1.0.6 (BD Biosciences, San Jose, California, USA). The experiment was repeated at least three times for both cell lines. (B) SPECTROPHOTOMETRY. The bar plot is a representative result where the experimental data are given as the arithmetic mean of the ratios of the red and the green JC-1 fluorescent signals with the standard deviation when the arithmetic mean of the ratios of DMSO-treated control cells was set as 100%. The experiment was repeated at least three times (Fig. SI-10) and four technical replicates were used for the determination of each experimental value.

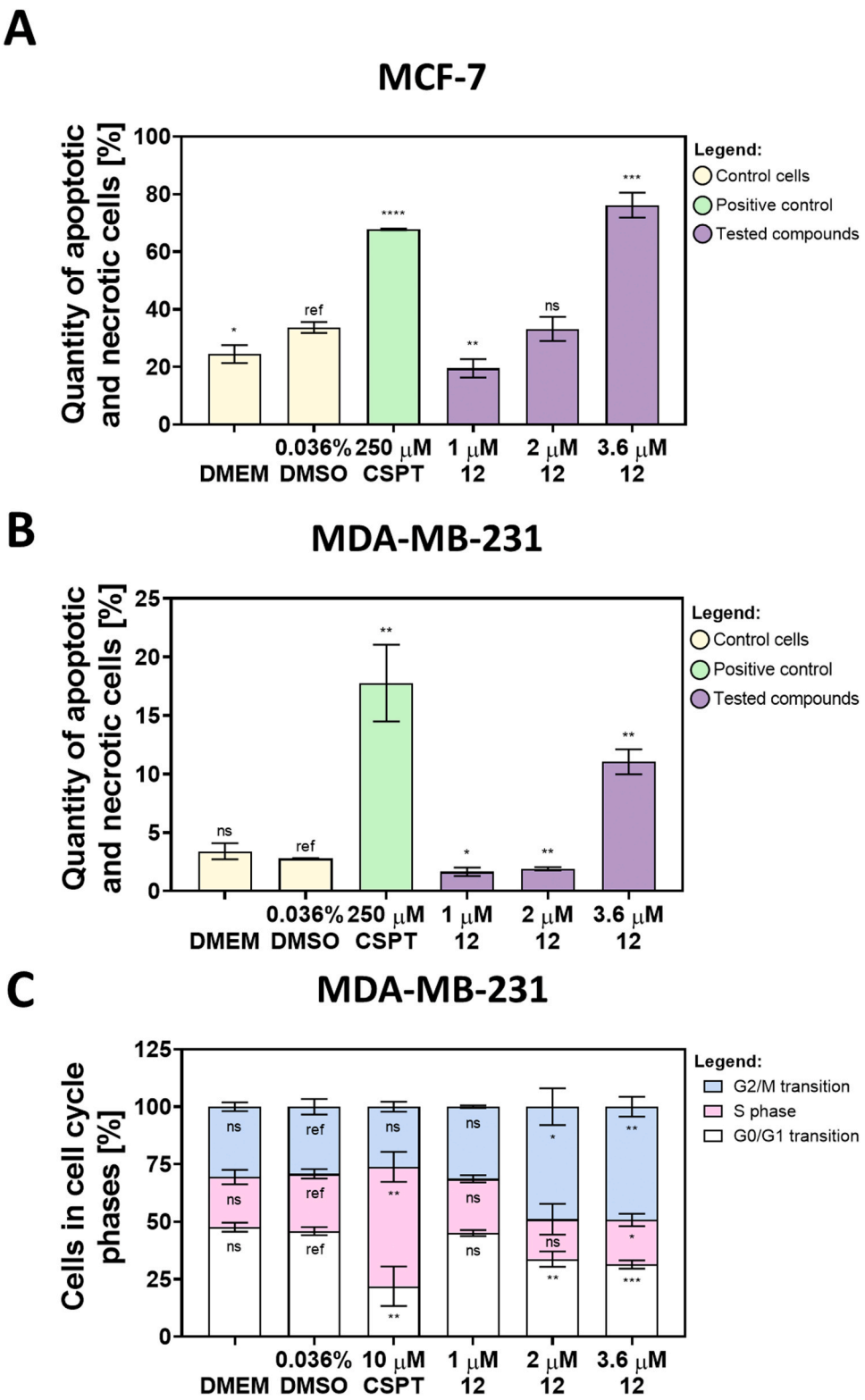

Fig. 6. Apoptosis and cell cycle analysis. (A, B) ANNEXIN V AND PI STAINING. (A) MCF7 or (B) MDA-MB-231 cells were treated with 12 and CSPT (positive control). The relative amount of necrotic/apoptotic cells after each treatment is displayed in bar graphs, where the obtained results are shown as relative changes in arithmetic means of three independent replicates, with error bars corresponding to the standard deviation. Representative graphs are displayed in Figure SI-7. The obtained experimental data were analysed using BD FACSuite™ software v1.0.6 (BD Biosciences, San Jose, California, USA). (C) PI STAINING OF MDA-MB-231 CELLS. Cell cycle analysis by flow cytometry were performed using PI. MDA-MB-231 cells were treated with **12** at three different concentrations (1 μM, 2 μM, or 3.6 μM). CSPT was used as a positive control responsible for blocking the cell cycle at the G2 phase. The distribution of cells in individual phases of the cell cycle was determined from fluorescence profiles (representative histograms are shown in Figure SI-9). Distribution statistic are displayed as the arithmetic mean of values from three independent measurements with standard deviation in stacked bar plots for a 24 h incubation period. Graphs for the other incubation times (48 and 72 h) are shown in Figure SI-9. BD FACSuite™ software v1.0.6 (BD Biosciences, San Jose, California, USA) was used for the analysis of experimental data.

in particular MitoTam, which successfully passed through a Phase 1 trial (MitoTam-01 trial; EudraCT 2017–004441–25) with promising outcomes, particularly for patients with metastatic renal cell carcinoma that responded very well to this treatment [38]. A Phase 2 trial with MitoTam is underway with a special focus on these patients [39]. MitoTam could also be used in monotherapy or combinatorial therapy with immune checkpoint inhibitors. Further, ongoing trials study SERD inhibitors because FLV, the only currently approved SERD, has limited bioavailability [40]. The most promising substances are elacestrant (RAD-1901) that is currently in a Phase 3 trial in ER+ /HER2- advanced breast cancer patients (ClinicalTrials.gov Identifier: NCT03778931), or camizestrant (AZD-9833) that is being tested in a Phase 3 trial in combination with palbociclib in ER-positive breast cancer patients with HER2 overexpression (ClinicalTrials.gov Identifier: NCT04711252). These

examples demonstrate that there is still an unmet medical need for novel more effective treatments with low or no side-effects.

High-throughput virtual *in silico* screening (HTVS) represents a powerful complement to experimental techniques, especially in preclinical research. Its main advantages are time- and cost-effectiveness compared to classical experimental methods. HTVS uses computational methods to screen large databases of virtual compounds. This screening is usually based on either similarity to a described inhibitor (ligand-based HTVS) or complementarity with a solved protein structure (structure-based HTVS) [41]. This enables the screening of large compound libraries to select a small group of promising ligands with a highly probable impact on a target structure such as protein receptor(s) verifiable by experimental methods [42]. This set-up has been successfully used in many recently published studies related to steroid research, such as articles studying monohydroxylated brassinosteroid analogues [43], brassinosteroid derivatives with a p-substituted phenyl group in the side chain [44], aryl brassinosteroids [45], and side chain analogues containing nitrogen [46]. In addition, HTVS based on molecular docking allows prediction of the binding position of the tested ligand, which could facilitate subsequent modification of the given compound [42].

Our structure-based virtual screening of the steroid compounds library identified a group of 15 candidates as potential ER ligands. The effect on the viability of breast cancer-derived cells was determined by the MTT assay and inhibitory activity towards ER by the dual luciferase assay. Based on this approach, compound **12** was selected as the most promising structure, showing efficacy comparable to commercial ER inhibitors such as TAM and FLV. We have defined a key structure motive of **12** as the double bond between carbons C15 and C16 in the D-ring of the steroid skeleton because the presence of the double bond is the only structural difference compared to E1, a natural ER agonist. This structural similarity causes **12** to occupy the ER cavity (Fig. 7 A) in the same manner as E2 [47]. The D-ring of both E1 and **12** contains an oxo group at carbon C17, which is essential for ER activation because it attracts α-helix H12 of ER by inducing a network of hydrogen bonds [48]. Perhaps the double bond conjugated with the oxo group can prevent the attraction of the α-helix H12. On the other hand, the oxo group *per se* at carbon C17 may undergo a 1,2-addition reaction. Moreover, we hypothesize that the double bond in the D-ring, due to conjugation with the oxo group, may stabilise the positive charge on the carbon C15 of the double bond by resonance (Fig. 7B). This structural motif can then easily undergo a 1,4-addition reaction. In both addition reactions, any nucleophile can be added to the positively charged carbon and, therefore, the oxygen functional group on carbon C17 may be in a position that is not suitable for ER activation, or may interfere with the closing of the ER cavity if long chains are added. The results from our study do not clarify which structural feature plays the key role in this process (it may not be just one), and further structure-activity relationship studies would be needed. However, western blotting analysis showed a clear decrease in PR expression, a well-known ER target gene [49–51], thereby confirming functional inhibition of ER activity by compound **12** similar to the commercial inhibitors used in this study.

Despite the same impact on PR, TAM and FLV represent two classes of ER inhibitors, the mechanisms of which are associated with the different stability of the formed ER-ligand complex. As a SERM, TAM creates an inactive complex with ER mainly due to the position of α-helix H12. Thereby, this induced conformation of the ER prevents its binding with co-regulators and at the same time leads to a decrease in ER transcriptional activity. However, this complex does not undergo degradation [23], as shown by an increased ER protein level in MCF7 cells (Fig. 3A), which is in agreement with published data of pituitary

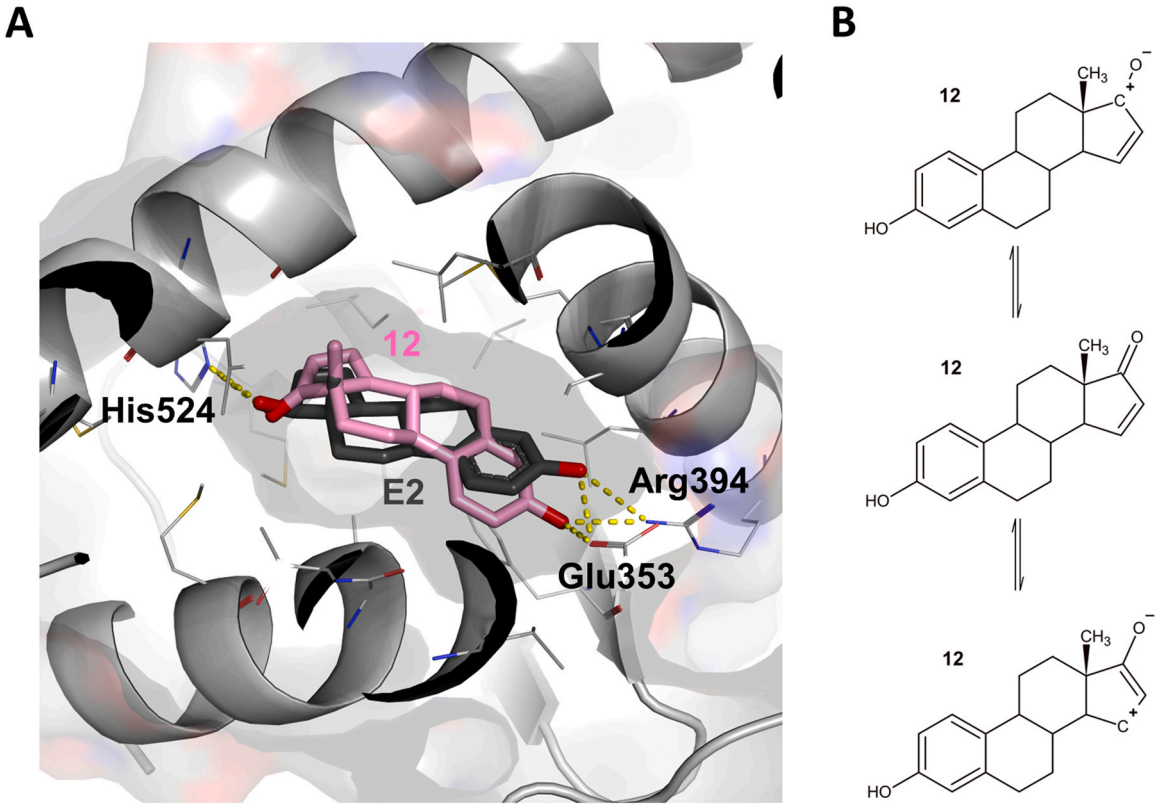

Fig. 7. (A) BINDING POSITION OF **12** INSIDE THE ER CAVITY. The structure of **12** (pink structure) is very similar to E2 (black structure) which also corresponds to its binding position in the ER cavity (PDB ID: 1X7R; [22]). Predicted hydrogen bonds are highlighted with yellow dashed lines. PyMOL software (The PyMOL Molecular Graphics System, Version 1.3, Schrödinger, LLC) was used to visualise the described structures. (B) RESONANCE STRUCTURES OF **12**. The double bond in the D-ring of structure **12** is conjugated to the oxo group at carbon C17. The described structural motif can have three resonance structures that increases the reactivity of this double bond.

lactotroph PR1 cells [52], ER-positive MCF7 breast cancer cells [53], or MDA-MB-231 human triple-negative breast cancer cells stably transfected with ER [54]. On the other hand, the interaction of FLV as a SERD with ER hinders ER dimerization, increases ER turnover, and disrupts ER nuclear localization [18,55]. The emerged complex is ubiquitinated and subsequently targeted for degradation by the proteasome [56,57]. To study the role of the proteasome in ER degradation in response to compound **12**, MCF7 cells were pre-treated with the proteasome inhibitors BZM or MG-132, and subsequently exposed to **12**. Proteasome inhibitors did not prevent ER degradation, indicating that compound **12** does not target ER via the proteasome degradation.

Although ER represents the main target of (anti)estrogens, various molecules including TAM can also exhibit nongenomic activity, including their interaction with mitochondrial structures [58]. For example, TAM as single agent or in combination with E2 causes mitochondrial dysfunction by acting through mitochondrial complex I [32], the mitochondrial complex II [35], and the mitochondrial complex III [33,34]. These findings have led to the development of new drugs and treatment strategies, such as combinatorial treatment HYPERTAM [59] or mitochondria-targeted TAM known as MitoTam [35]. Compound **12** decreased the viability of both ER-positive and ER-negative breast cancer cells indicating that **12** targets both ER and mitochondria. Indeed, JC-1 staining confirmed that **12** also influences the $\Delta\Psi m$ representing the energetic state of mitochondria. Changes in $\Delta\Psi m$ were detected in both cell lines and were even higher in MCF7 cells, which may reflect a different metabolic and redox activity of these cells compared to MDA-MB-231 cells [34]. Interestingly, although the structure of MitoTam is based on TAM, the chemical modification prevents interactions between MitoTam and ER, unlike **12**, which exhibits a dual mode of action.

Commonly used antiestrogens such as TAM [60] or FLV [61] usually induce cell cycle block at the G1 phase, leading to inhibition of cellular proliferation [62]. Here, we investigated the impact of **12** on the cell cycle. Interestingly, treatment with **12** significantly influenced only MDA-MB-231 cells by inducing cell cycle arrest in the G2 phase. On the other hand, it has also been reported that some compounds reducing ER activity could also block the cell cycle at the G2 phase independently of their effect on ER. For example, the phytoestrogen genistein causes G1/G0 arrest of pancreatic cancer cell lines Mia-PaCa2 and PANC-1 [63]. In contrast, in T24 human bladder cancer cells [64], and human leukaemia cells HL-60, genistein induces a G2/M block [65]. Quercetin, some flavonoid found in many fruits, vegetables, seeds, and nuts, also shows anti-estrogenic activity [66], which is associated with G0/G1 arrest of HL-60 cells [67] or G2/M phase in MCF7, U937, and OE33 cells [68–70]. Importantly, antiestrogens such as TAM or FLV can induce cell cycle arrest as well as apoptosis; however, the function of estrogen signaling as a link between these biological processes and their signaling pathways is not fully understood [71–73]. It is generally known that apoptosis and cell cycle arrest share the same genes or molecules in their signalling pathways [68,74]. An example is the tumour suppressor protein p53, which can act in both processes mainly through the transactivation of molecules such as p21, Gadd45, Mdm2, cyclin D1, Bax, Bcl-xL, FasL, etc. [74,75]. Moreover, there is a growing evidence that distinct types of p53 mutations have various functional implications associated with different clinical impacts [76]. Along with cellular backgrounds, these various effects may also be associated with the doses of the applied drug, as has been demonstrated for TAM. While the application of TAM at lower concentrations (0.1–1 μM) induces cell cycle arrest [77], pharmacological concentrations of TAM (above 5 μM) induce apoptosis [78]. This dose-dependent impact on cancer cells is related to its nongenomic effects that are ER-independent, as was demonstrated in various tumor cells such as T-leukemic Jurkat cells, ovarian cancer cells A2780 [58], HepG2 human hepatoblastoma cells [79], rat C6 glioma cells, human ER-positive MCF7 [80], and ER-negative breast cancer cell lines MDA-MB-231, MDA-MB-468, MDA-MB-453, and SK-BR-3 [81]. Compared to TAM, FLV induces apoptosis only in ER-positive breast tumours as demonstrated in MCF7 or T-47D cells [82,83]. Interestingly, based on our Annexin V/PI staining results, treatment with **12** induced apoptosis in both cell lines, supporting the hypothesis of multiple mechanisms of action.

Another important issue to be discussed is the ER as a target modulated by estrogens leading to induction of apoptosis. Jordan et al. proposed two molecular classes of estrogens: planar and angular, which induce apoptosis in different ways depending on the resulting conformation of the ER complex [84]. Briefly, class I planar estrogens (e.g. estradiol, allowing for helix 12 closure) trigger apoptosis after 24 h whereas class II angular estrogens (e.g. bisphenol triphenylethylene, do not allowing for helix 12 closure) delay the process until after 72 h [85]. Consistent with this, we observed a significant dose-dependent decrease in the metabolic activity of MCF7 cells exposed to **12** as early as 24 h (Fig. SI-14), which could also be related to the induction of apoptosis observed in response to compound **12** (Fig. 6A). Thus, even this alternative mechanism responsible for the induction of apoptosis cannot be completely ruled out. However, under our conditions, tumor cells were not exposed to long-term E2 deprivation and an antagonistic effect of compound **12** can be rather considered.

5. Summary and conclusions

This article describes the effect of compound **12** on MCF7 and MDA-MB-231 breast cancer cell lines. This derivative was chosen based on the combination of computational and experimental methods representing a rapid methodology to investigate the activity of small compounds libraries. In our study, this approach led to the identification of compound **12** as an ER antagonist, most likely due to the presence of the double bond in the D-ring conjugated with the C17 oxo group. Interestingly, mitochondria represent the second molecular target of **12**. These findings indicate a dual mechanism of action associated with reduced breast cancer cells viability independent of hormonal receptor status. These interesting and promising properties make compound **12** worthy of further research.

Declaration of Competing Interest

The authors declare that they have no known competing financial interests or personal relationships that could have appeared to influence the work reported in this paper.

Data availability

Data will be made available on request.

Acknowledgements and additional information

We would especially like to thank Dr. Philip John Coates (https://orcid.org/0000–0003-1518–6306) for proofreading this article. This work was supported by the National Institute for Cancer Research (Programme EXCELES, ID Project No. LX22NPO5102), MH CZ DRO (MMCI, 00209805), ASCR (RVO: 61388963) and by the Ministry of Education, Youth and Sports of the Czech Republic through the e-INFRA CZ (ID:90140), ELIXIR-CZ no. LM2023055 and BBMRI.cz no. LM2023033.

Appendix A. Supporting information

Supplementary data associated with this article can be found in the online version at doi:10.1016/j.jsbmb.2023.106365.

References

[1] H. Sung, J. Ferlay, R.L. Siegel, M. Laversanne, I. Soerjomataram, A. Jemal, et al., Global cancer statistics 2020: GLOBOCAN estimates of incidence and mortality worldwide for 36 cancers in 185 countries, CA A Cancer J. Clin. 71 (2021) 209–249.

[2] J. Cuzick, M. Dowsett, S. Pineda, C. Wale, J. Salter, E. Quinn, et al., Prognostic value of a combined estrogen receptor, progesterone receptor, Ki-67, and human epidermal growth factor receptor 2 immunohistochemical score and comparison with the Genomic Health Recurrence Score in Early Breast Cancer, JCO 29 (2011) 4273–4278.

[3] A. Goldhirsch, E.P. Winer, A.S. Coates, R.D. Gelber, M. Piccart-Gebhart, B. Thürlimann, et al., Personalizing the treatment of women with early breast cancer: highlights of the St Gallen International Expert Consensus on the Primary Therapy of Early Breast Cancer 2013, Ann. Oncol. 24 (2013) 2206–2223.

[4] C.M. Perou, T. Sørlie, M.B. Eisen, M. van de Rijn, S.S. Jeffrey, C.A. Rees, et al., Molecular portraits of human breast tumours, Nature 406 (2000) 747–752.

[5] T. Sørlie, C.M. Perou, R. Tibshirani, T. Aas, S. Geisler, H. Johnsen, et al., Gene expression patterns of breast carcinomas distinguish tumor subclasses with clinical implications, Proc. Natl. Acad. Sci. USA 98 (2001) 10869–10874.

[6] S.K. Chia, V.H. Bramwell, D. Tu, L.E. Shepherd, S. Jiang, T. Vickery, et al., A 50-gene intrinsic subtype classifier for prognosis and prediction of benefit from adjuvant tamoxifen, Clin. Cancer Res. 18 (2012) 4465–4472.

[7] J. Liang, Y. Shang, Estrogen and cancer, Annu Rev. Physiol. 75 (2013) 225–240.

[8] S.F. Doisneau-Sixou, C.M. Sergio, J.S. Carroll, R. Hui, E.A. Musgrove, R. L. Sutherland, Estrogen and antiestrogen regulation of cell cycle progression in breast cancer cells, Endocr. -Relat. Cancer (2003) 179–186.

[9] T. Traboulsi, M. El Ezzy, J.L. Gleason, S. Mader, Antiestrogens: structure-activity relationships and use in breast cancer treatment, J. Mol. Endocrinol. 58 (2017) R15–R31.

[10] M.J.K. Harper, A.L.A. Walpole, New derivative of triphenylethylene: effect on implantation and mode of action in rats, Reproduction 13 (1967) 101–119.

[11] Cole M.P., Jones C.T.A., Todd I.D.H.A. NEW ANTI-OESTROGENIC AGENT I.N. LATE BREAST CANCER. British Journal of Cancer. 1971;25:270–275.

[12] H.W.C. Ward, Anti-oestrogen therapy for breast cancer: a trial of tamoxifen at two dose levels, BMJ 1 (1973) 13–14.

[13] B. Kristensen, B. Ejlertsen, P. Dalgaard, L. Larsen, S.N. Holmegaard, I. Transbøl, et al., Tamoxifen and bone metabolism in postmenopausal low-risk breast cancer patients: a randomized study, JCO 12 (1994) 992–997.

[14] T.J. Powles, T. Hickish, J.A. Kanis, A. Tidy, S. Ashley, Effect of tamoxifen on bone mineral density measured by dual-energy x-ray absorptiometry in healthy premenopausal and postmenopausal women, JCO 14 (1996) 78–84.

[15] R.R. Love, D.A. Wiebe, J.M. Feyzi, P.A. Newcomb, R.J. Chappell, Effects of tamoxifen on cardiovascular risk factors in postmenopausal women after 5 years of treatment, JNCI J. Natl. Cancer Inst. 86 (1994) 1534–1539.

[16] K.-C. An, Selective estrogen receptor modulators, Asian Spine J. 10 (2016) 787–791.

[17] A.E. Wakeling, M. Dukes, J. Bowler, A potent specific pure antiestrogen with clinical potential, Cancer Res. 51 (1991) 3867–3873.

[18] A. Howell, C.K. Osborne, C. Morris, A.E. Wakeling, ICI 182,780 (Faslodex): Development of a novel, "pure" antiestrogen, Cancer 89 (2000) 817–825.

[19] M. Fan, R.M. Bigsby, K.P. Nephew, The NEDD8 pathway is required for proteasome-mediated degradation of human estrogen receptor (ER)-α and essential for the antiproliferative activity of ICI 182,780 in ERα-positive breast cancer cells, Mol. Endocrinol. 17 (2003) 356–365.

[20] Ahmad I. Shagufta, S. Mathew, S. Rahman, Recent progress in selective estrogen receptor downregulators (SERDs) for the treatment of breast cancer, RSC Med Chem 11 (2020) 438–454.

[21] Cherinka B., Andrews B.H., Sánchez-Gallego J., Brownstein J., Argudo-Fernández M., Blanton M., et al. Marvin: A Tool Kit for Streamlined Access and Visualization of the SDSS-IV MaNGA Data Set. AJ. 2019;158:74.

[22] E.S. Manas, Z.B. Xu, R.J. Unwalla, W.S. Somers, Understanding the selectivity of genistein for human estrogen receptor-β using X-ray crystallography and computational methods, Structure 12 (2004) 2197–2207.

[23] A.K. Shiau, D. Barstad, P.M. Loria, L. Cheng, P.J. Kushner, D.A. Agard, et al., The structural basis of estrogen receptor/coactivator recognition and the antagonism of this interaction by tamoxifen, Cell 95 (1998) 927–937.

[24] G.M. Morris, R. Huey, W. Lindstrom, M.F. Sanner, R.K. Belew, D.S. Goodsell, et al., AutoDock4 and AutoDockTools4: Automated docking with selective receptor flexibility, J. Comput. Chem. 30 (2009) 2785–2791.

[25] O. Trott, A.J. Olson, AutoDock Vina: Improving the speed and accuracy of docking with a new scoring function, efficient optimization, and multithreading, J. Comput. Chem. 31 (2010) 455–461.

[26] T. Hodík, M. Lamač, L. Červenková Šťastná, J. Karban, L. Koubková, R. Hrstka, et al., Titanocene dihalides and ferrocenes bearing a pendant α-D-Xylofuranos-5-yl or α-D-Ribofuranos-5-yl Moiety. synthesis, characterization, and cytotoxic activity, Organometallics 33 (2014) 2059–2070.

[27] H. Skoupilova, M. Bartosik, L. Sommerova, J. Pinkas, T. Vaculovic, V. Kanicky, et al., Ferrocenes as new anticancer drug candidates: Determination of the mechanism of action, Eur. J. Pharmacol. 867 (2020), 172825.

[28] P. Narasimha, A. Hameed, H. Moore, Conjugates. specific antisera for radioimmunoassay of 5a-dihydrotestosterone, 5a-androstane-3fl,17P_diol and 5a-androstane-3a,17P_DIOL, Steroids 29 (1977) 171–184.

[29] Ferreiro Gil J.J., Iglesias Retuerto J.M., Gallo Nieto F.J. Process for the preparation of estetrol.

[30] N.M. Hamilton, M. Dawson, E.E. Fairweather, N.S. Hamilton, J.R. Hitchin, D. I. James, et al., Novel steroid inhibitors of glucose 6-phosphate dehydrogenase, J. Med Chem. 55 (2012) 4431–4445.

[31] C.A. Schneider, W.S. Rasband, K.W. Eliceiri, NIH Image to ImageJ: 25 years of image analysis, Nat. Methods 9 (2012) 671–675.

[32] P.I. Moreira, J. Custódio, A. Moreno, C.R. Oliveira, M.S. Santos, Tamoxifen and estradiol interact with the flavin mononucleotide site of complex i leading to mitochondrial failure, J. Biol. Chem. 281 (2006) 10143–10152.

[33] T.A. Theodossiou, K. Yannakopoulou, C. Aggelidou, J.S. Hothersall, Tamoxifen subcellular localization; observation of cell-specific cytotoxicity enhancement by inhibition of mitochondrial ETC complexes I and III, Photochem. Photobiol. 88 (2012) 1016–1022.

[34] T.A. Theodossiou, S. Wälchli, C.E. Olsen, E. Skarpen, K. Berg, Deciphering the nongenomic, mitochondrial toxicity of tamoxifens as determined by cell metabolism and redox activity, ACS Chem. Biol. 11 (2016) 251–262.

[35] K. Rohlenova, K. Sachaphibulkij, J. Stursa, A. Bezawork-Geleta, J. Blecha, B. Endaya, et al., Selective disruption of respiratory supercomplexes as a new strategy to suppress Her2 ^{high} breast cancer, Antioxid. Redox Signal. 26 (2017) 84–103.

[36] E. Gottlieb, S.M. Armour, M.H. Harris, C.B. Thompson, Mitochondrial membrane potential regulates matrix configuration and cytochrome c release during apoptosis, Cell Death Differ. 10 (2003) 709–717.

[37] S. JavanMoghadam, Z. Weihua, K.K. Hunt, K. Keyomarsi, Estrogen receptor alpha is cell cycle-regulated and regulates the cell cycle in a ligand-dependent fashion, Cell Cycle 15 (2016) 1579–1590.

[38] S. Stemberkova-Hubackova, R. Zobalova, M. Dubisova, J. Smigova, S. Dvorakova, K. Korinkova, et al., Simultaneous targeting of mitochondrial metabolism and immune checkpoints as a new strategy for renal cancer therapy, Clin. Transl. Med 12 (2022), e645.

[39] L. Dong, V. Gopalan, O. Holland, J. Neuzil, Mitocans revisited: mitochondrial targeting as efficient anti-cancer therapy, IJMS 21 (2020) 7941.

[40] Y.-C. Chen, J. Yu, C. Metcalfe, T. De Bruyn, T. Gelzleichter, V. Malhi, et al., Latest generation estrogen receptor degraders for the treatment of hormone receptor-positive breast cancer, Expert Opin. Investig. Drugs 31 (2022) 515–529.

[41] B.K. Shoichet, Virtual screening of chemical libraries, Nature 432 (2004) 862–865.

[42] P. Ripphausen, B. Nisius, J. Bajorath, State-of-the-art in ligand-based virtual screening, Drug Discov. Today 16 (2011) 372–376.

[43] M. Kvasnica, J. Oklestkova, V. Bazgier, L. Rarova, K. Berka, M. Strnad, Biological activities of new monohydroxylated brassinosteroid analogues with a carboxylic group in the side chain, Steroids 85 (2014) 58–64.

[44] M. Kvasnica, J. Oklestkova, V. Bazgier, L. Rárová, P. Korinkova, J. Mikulík, et al., Design, synthesis and biological activities of new brassinosteroid analogues with a phenyl group in the side chain, Org. Biomol. Chem. 14 (2016) 8691–8701.

[45] P. Korinkova, V. Bazgier, J. Oklestkova, L. Rarova, M. Strnad, M. Kvasnica, Synthesis of novel aryl brassinosteroids through alkene cross-metathesis and preliminary biological study, Steroids 127 (2017) 46–55.

[46] M.V. Diachkov, K. Ferrer, J. Oklestkova, L. Rarova, V. Bazgier, M. Kvasnica, Synthesis and biological activity of brassinosteroid analogues with a nitrogen-containing side chain, IJMS 22 (2020) 155.

[47] M. Pavlin, A. Spinello, M. Pennati, N. Zaffaroni, S. Gobbi, A. Bisi, et al., A computational assay of estrogen receptor α antagonists reveals the key common structural traits of drugs effectively fighting refractory breast cancers, Sci. Rep. 8 (2018) 649.

[48] A.M. Brzozowski, A.C.W. Pike, Z. Dauter, R.E. Hubbard, T. Bonn, O. Engström, et al., Molecular basis of agonism and antagonism in the oestrogen receptor, Nature 389 (1997) 753–758.

[49] W. Toy, Y. Shen, H. Won, B. Green, R.A. Sakr, M. Will, et al., ESR1 ligand-binding domain mutations in hormone-resistant breast cancer, Nat. Genet 45 (2013) 1439–1445.

[50] W. Toy, H. Weir, P. Razavi, M. Lawson, A.U. Goeppert, A.M. Mazzola, et al., Activating *ESR*1 mutations differentially affect the efficacy of ER antagonists, Cancer Discov. 7 (2017) 277–287.

[51] R. Cheng, L. Qi, X. Kong, Z. Wang, Y. Fang, J. Wang, Identification of the significant genes regulated by estrogen receptor in estrogen receptor-positive breast cancer and their expression pattern changes when tamoxifen or fulvestrant resistance occurs, Front Genet 11 (2020), 538734.

[52] M.T. Preisler-Mashek, N. Solodin, B.L. Stark, M.K. Tyriver, E.T. Alarid, Ligand-specific regulation of proteasome-mediated proteolysis of estrogen receptor-α, Am. J. Physiol. Endocrinol. Metab. 282 (2002) E891–E898.

[53] G.L. Powers, S.J. Ellison-Zelski, A.J. Casa, A.V. Lee, E.T. Alarid, Proteasome inhibition represses ERα gene expression in ER+ cells: a new link between proteasome activity and estrogen signaling in breast cancer, Oncogene 29 (2010) 1509–1518.

[54] S.T. Pearce, H. Liu, V.C. Jordan, Modulation of estrogen receptor α function and stability by tamoxifen and a critical amino acid (Asp-538) in Helix 12, J. Biol. Chem. 278 (2003) 7630–7638.

[55] R.A. McClelland, D.L. Manning, J.M.W. Gee, E. Anderson, R. Clarke, A. Howell, et al., Effects of short-term antiestrogen treatment of primary breast cancer on estrogen receptor mRNA and protein expression and on estrogen-regulated genes, Breast Cancer Res Tr. 41 (1996) 31–41.

[56] G. Reid, M.R. Hübner, R. Métivier, H. Brand, S. Denger, D. Manu, et al., Cyclic, proteasome-mediated turnover of unliganded and liganded ER_ on responsive promoters is an integral feature of estrogen signaling, Mol. Cell 11 (2003) 695–707.

[57] A.J. Casa, D. Hochbaum, S. Sreekumar, S. Oesterreich, A.V. Lee, The estrogen receptor alpha nuclear localization sequence is critical for fulvestrant-induced degradation of the receptor, Mol. Cell. Endocrinol. 415 (2015) 76–86.

[58] C. Ferlini, G. Scambia, M. Marone, M. Distefano, C. Gaggini, G. Ferrandina, et al., Tamoxifen induces oxidative stress and apoptosis in oestrogen receptor-negative human cancer cell lines, Br. J. Cancer 79 (1999) 257–263.

[59] T.A. Theodossiou, M. Ali, M. Grigalavicius, B. Grallert, P. Dillard, K.O. Schink, et al., Simultaneous defeat of MCF7 and MDA-MB-231 resistances by a hypericin PDT–tamoxifen hybrid therapy, npj Breast Cancer 5 (2019) 13.
[60] N.S. Yaacob, N.N.N.M. Kamal, K.K. Wong, M.N. Norazmi, Cell cycle modulation of MCF-7 and MDA-MB-231 by a sub-fraction of strobilanthes crispus and its combination with tamoxifen, Asian Pac. J. Cancer Prev. 16 (2016) 8135–8140.
[61] S. Somaï, M. Chaouat, D. Jacob, J.-Y. Perrot, W. Rostène, P. Forgez, et al., Antiestrogens are pro-apoptotic in normal human breast epithelial cells, Int. J. Cancer 105 (2003) 607–612.
[62] C. Hurd, N. Khattree, S. Dinda, P. Alban, V.K. Moudgil, Regulation of tumor suppressor proteins, p53 and retinoblastoma, by estrogen and antiestrogens in breast cancer cells, Oncogene 15 (1997) 991–995.
[63] Y. Bi, M. Min, W. Shen, Y. Liu, Genistein induced anticancer effects on pancreatic cancer cell lines involves mitochondrial apoptosis, G 0 /G 1 cell cycle arrest and regulation of STAT3 signalling pathway, Phytomedicine 39 (2018) 10–16.
[64] Cha Park, Hwang-Bo Lee, Kim Ji, et al., Induction of G2/M cell cycle arrest and apoptosis by genistein in human bladder cancer T24 cells through inhibition of the ROS-dependent PI3k/Akt signal transduction pathway, Antioxidants 8 (2019) 327.
[65] Y.-C. Hsiao, S.-F. Peng, K.-C. Lai, C.-L. Liao, Y.-P. Huang, C.-C. Lin, et al., Genistein induces apoptosis in vitro and has antitumor activity against human leukemia HL-60 cancer cell xenograft growth in vivo, Environ. Toxicol. 34 (2019) 443–456.
[66] H. van der Woude, M.G.R. ter Veld, N. Jacobs, P.T. van der Saag, A.J. Murk, I.M.C. M. Rietjens, The stimulation of cell proliferation by quercetin is mediated by the estrogen receptor, Mol. Nutr. Food Res 49 (2005) 763–771.
[67] Z. Yuan, C. Long, T. Junming, L. Qihuan, Z. Youshun, Z. Chan, Quercetin-induced apoptosis of HL-60 cells by reducing PI3K/Akt, Mol. Biol. Rep. 39 (2012) 7785–7793.
[68] J.-A. Choi, J.-Y. Kim, J.-Y. Lee, C.-M. Kang, H.-J. Kwon, Y.-D. Yoo, et al., Induction of cell cycle arrest and apoptosis in human breast cancer cells by quercetin, Int J. Oncol. 19 (2001) 837–844.
[69] T.-J. Lee, O.H. Kim, Y.H. Kim, J.H. Lim, S. Kim, J.-W. Park, et al., Quercetin arrests G2/M phase and induces caspase-dependent cell death in U937 cells, Cancer Lett. 240 (2006) 234–242.
[70] Q. Zhang, X.-H. Zhao, Z.-J. Wang, Flavones and flavonols exert cytotoxic effects on a human oesophageal adenocarcinoma cell line (OE33) by causing G2/M arrest and inducing apoptosis, Food Chem. Toxicol. 46 (2008) 2042–2053.
[71] K.B. Bouker, T.C. Skaar, D.R. Fernandez, K.A. O'Brien, R.B. Riggins, D. Cao, et al., Interferon regulatory factor-1 mediates the proapoptotic but not cell cycle arrest effects of the steroidal antiestrogen ICI 182,780 (Faslodex, Fulvestrant), Cancer Res. 64 (2004) 4030–4039.
[72] J. Gauduchon, F. Gouilleux, S. Maillard, V. Marsaud, J.-M. Renoir, B. Sola, 4-Hydroxytamoxifen Inhibits proliferation of multiple myeloma cells *In vitro* through down-regulation of c-Myc, up-regulation of p27Kip1, and modulation of Bcl-2 family members, Clin. Cancer Res. 11 (2005) 2345–2354.
[73] J.-M. Renoir, C. Bouclier, A. Seguin, V. Marsaud, B. Sola, Antioestrogen-mediated cell cycle arrest and apoptosis induction in breast cancer and multiple myeloma cells, J. Mol. Endocrinol. 40 (2008) 101–112.
[74] F.Q.B. Alenzi, Links between apoptosis, proliferation and the cell cycle, Br. J. Biomed. Sci. 61 (2004) 99–102.
[75] J. Pflaum, S. Schlosser, M. Müller, p53 family and cellular stress responses in cancer, Front Oncol. 4 (2014) 285.
[76] P. Dobes, J. Podhorec, O. Coufal, A. Jureckova, K. Petrakova, B. Vojtesek, et al., Influence of mutation type on prognostic and predictive values of TP53 status in primary breast cancer patients, Oncol. Rep. 32 (2014) 1695–1702.
[77] A.M. Otto, R. Paddenberg, S. Schubert, H.G. Mannherz, Cell-cycle arrest, micronucleus formation, and cell death in growth inhibition of MCF-7 breast cancer cells by tamoxifen and cisplatin, J. Cancer Res Clin. Oncol. 122 (1996) 603–612.
[78] R.R. Perry, Y. Kang, B. Greaves, Effects of tamoxifen on growth and apoptosis of estrogen-dependent and -independent human breast cancer cells, Ann. Surg. Oncol. 2 (1995) 238–245.
[79] J.-A. Kim, Y.S. Kang, M.-W. Jung, S.H. Lee, Y.S. Lee, Involvement of Ca2+ influx in the mechanism of tamoxifen-induced apoptosis in HepG2 human hepatoblastoma cells, Cancer Lett. 147 (1999) 115–123.
[80] W. Zhang, W.T. Couldwell, H. Song, T. Takano, J.H.C. Lin, M. Nedergaard, Tamoxifen-induced enhancement of calcium signaling in glioma and MCF-7 breast cancer cells, Cancer Res. 60 (2000) 5395–5400.
[81] C.-Y. Liu, M.-H. Hung, D.-S. Wang, P.-Y. Chu, J.-C. Su, T.-H. Teng, et al., Tamoxifen induces apoptosis through cancerous inhibitor of protein phosphatase 2A–dependent phospho-Akt inactivation in estrogen receptor–negative human breast cancer cells, Breast Cancer Res 16 (2014) 431.
[82] P.A. Ellis, G. Saccani-Jotti, R. Clarke, S.R.D. Johnston, E. Anderson, A. Howell, et al., Induction of apoptosis by tamoxifen and ICI 182780 in primary breast cancer, Int J. Cancer 72 (1997) 608–613.
[83] G.H. Jansen, H.R. Franke, F. Wolbers, M. Brinkhuis, I. Vermes, Effects of fulvestrant alone or combined with different steroids in human breast cancer cells in vitro, Climacteric 11 (2008) 315–321.
[84] V.C. Jordan, J.M. Schafer, A.S. Levenson, H. Liu, K.M. Pease, L.A. Simons, et al., Molecular classification of estrogens, Cancer Res 61 (2001) 6619–6623.
[85] V.C. Jordan, The new biology of estrogen-induced apoptosis applied to treat and prevent breast cancer, Endocr. Relat. Cancer 22 (2015) R1–R31.